buildings

MDPI

Article

Rising Damp Treatment in Historical Buildings by Electro-Osmosis: A Case Study

Aliihsan Koca [1,*], Mehmet Nurettin Uğural [2] and Ergün Yaman [2]

[1] Department of Mechanical Engineering, Istanbul Technical University, Gumussuyu, 34437 Istanbul, Türkiye
[2] Faculty of Engineering, Istanbul Kultur University, 34140 Istanbul, Türkiye; m.ugural@iku.edu.tr (M.N.U.); 1700004183@stu.iku.edu.tr (E.Y.)
* Correspondence: ihsankoca@hotmail.com or akoca@itu.edu.tr

Abstract: Throughout the past century, numerous technologies have been suggested to deal with the capillary rise of water through the soil in historic masonry buildings. The aim of this study was to examine the effectiveness of capillary moisture repulsion apparatus that uses the electro-osmosis approach over a prolonged period of time. The Gül mosque was selected as a sample historical building affected by structural problems caused by the absorption of water through small channels on its walls due to capillary action. The moisture repulsion mechanism efficiently decreased the moisture level in the walls from a 'wet' state to a 'dry' state in roughly 9 months. After the installation of the equipment, the water mass ratio of the building decreased from 14.48% to 2.90%. It was determined that the majority of the water in the building was relocated during the initial measurement period. Furthermore, it inhibited the absorption of water by capillary action by protecting the construction elements that were in contact with the wet ground. Lastly, capillary water repulsion coefficients (C) for various measurement durations and time factors were proposed. The average value of C was calculated to be 0.152 kg/m^2 s$^{0.5}$ by measuring the point at which the water repulsion remained nearly constant.

Keywords: rising damp; electro-osmosis; humidity; capillarity; masonry; construction; project management

check for updates

Citation: Koca, A.; Uğural, M.N.; Yaman, E. Rising Damp Treatment in Historical Buildings by Electro-Osmosis: A Case Study. *Buildings* **2024**, *14*, 1460. https://doi.org/10.3390/buildings14051460

Received: 6 April 2024
Revised: 7 May 2024
Accepted: 8 May 2024
Published: 17 May 2024

Copyright: © 2024 by the authors. Licensee MDPI, Basel, Switzerland. This article is an open access article distributed under the terms and conditions of the Creative Commons Attribution (CC BY) license (https://creativecommons.org/licenses/by/4.0/).

1. Introduction

Rising damp is a significant issue that significantly impacts historic masonry buildings, resulting in undesirable effects such as poor indoor conditions characterized by elevated relative air humidity as well as the corrosion of materials [1]. The presence of moisture in the pores of materials, together with other environmental conditions, can result in biological degradation, salt crystallization, chemical degradation, swelling in clay-bearing stones, frost damage, and ultimately material loss and structural issues [2]. Rising damp is a prevalent occurrence in old buildings, caused by the presence of water in the ground near the masonry. This phenomenon has been extensively investigated for a considerable period of time [3]. The presence of dampness can be attributed to the lack of impermeable sheets and/or the inadequacy of conventional 'waterproofing applications' such as the use of densely packed stones during construction near the ground [4,5]. The upward movement of water in a vertical capillary vessel submerged in a water basin is attributed to the capillary forces that occur between the water and the surface of the solid. This phenomenon is primarily influenced by the strong wettability of solid surfaces, as evidenced by the minimal contact angle between a fluid and solid. This phenomenon has been observed in the context of hydrophilic substances [1]. Water capillary rise is considered a crucial factor in heritage conservation due to its significant impact on masonries. Numerous literature studies have been dedicated to studying the principles of water capillary rise from the ground [6,7], its negative consequences, and methods to evaluate moisture absorption in buildings [8–10].

Damp walls have been found to result in elevated levels of indoor relative humidity in the air and the development of mold on cold surfaces, generating unfavorable indoor conditions [11]. Consequently, this has a detrimental impact on the air quality and subsequently affects the health of occupants. The thermal insulation property of building materials is adversely impacted by the presence of water within their pores. It has been estimated that a 1 wt% rise in water content can lead to a 5% rise in the coefficient of thermal conductivity of masonry [12]. Consequently, porous stones and bricks may even experience a 100% increase in thermal conductivity as a result of the level of saturation. The compressive and shear strength of construction materials are adversely impacted by the existence of water within their pores [13]. Rising damp is a contributing factor to the deterioration of historical building materials, including the disintegration of paints, ceramic tiles, mosaics, and other similar components [14].

Numerous methodologies have been suggested in order to mitigate water infiltration or diminish the moisture level within masonry. Classical techniques depend on implementing physical obstacles to prevent water from entering or facilitating the evaporation of water through masonry [15–17]. Within the realm of dehumidification procedures, there exist approaches that rely on the circulation of an electric current through the masonry, harnessing electroosmotic phenomena. Typically, these procedures necessitate the placement of electrodes in both the damp wall and at a distant location, usually in the soil. The electrical current is typically supplied to the electrode located within the masonry, serving as the anode, while the remote electrode functions as the cathode. This arrangement facilitates the movement of water towards the cathode, resulting in a decrease in the moisture content within the masonry. The basis of this technique lies in the electrokinetic hypothesis regarding electro-osmosis, which posits that the flow of a liquid phase into pores can be generated by a direct current passing through a saturated material that is porous. The transportation of water exhibits a correlation with both the magnitude of the voltage differential and the characteristics of the porous substance. The phenomenon of electro-osmotic flow arises from the electrical engagement occurring between the solid phase's surface and the liquid, resulting in the separation of charges at the interface. Electro-osmosis is influenced by the characteristics of the double layer, which in turn is influenced by the chemical formula of the porous substance and the pore solution. Additionally, the shape and size of the pores play a role in determining electro-osmosis. Water often flows in a similar direction to the electric current, specifically from the anode to the cathode [18].

The technology of electro-osmosis has been applied to clay soils—for example, to humidify dry soil or, on the other hand, to consolidate wet soils. Evidence of water movement and variations in soil humidity has been presented in this instance [19]. However, there are no comparable experimental demonstrations for use with building materials [20]. There is a dearth of quantitative data in the technical literature on humidity changes following the implementation of dehumidification procedures, which is crucial for the proper assessment of their real performance [15]. Through the implantation of an external DC electric field, active electro-osmosis is predicted to trigger the transport of water in the small holes from the electrodes utilized in the damp wall (anode) to the electrodes attached to the ground (cathode). Utilizing the electrokinetic processes associated with water movement in porous materials, electro-osmosis has been widely used to regulate the moisture content of clay soils [21]. A few studies have examined the phenomenon of water movement by electro-osmosis in various construction materials [15–22]. A variety of researchers have expressed disapproval of this approach since it lacks experimental validation [3], produces conflicting results that make it impossible to advocate for its use [23], and has had little success in field implementation [24].

The damage produced by migrating salts in older buildings with rising moisture was examined by Torres and Freitas [25]. Studies on 20 cm limestone walls have shown that the best treatment is the ventilation of the wall base. Nevertheless, the effects of varying wall compositions and thicknesses remain unknown. The University of Coimbra and Porto performed a numerical analysis, which is presented in their work, to examine how

the wall thickness and composition affect how well ventilation works to address rising damp in historical walls. The goal of the study was to increase the treatment method's potential applications. Zhang and Nowamooz examined a subject that has received little attention in the literature: the effect of rising damp on the thermal–hydromechanical (THM) mechanisms of unstabilized masonry buildings. The study compared damp-affected and dry walls using finite element analysis and a theoretical framework that has been validated. The findings demonstrate that while increasing damp cools walls and speeds up drying and water flow downhill, time improves the THM characteristics in dry walls by evaporation. The horizontal capacity for bearing grew by 47% without damp over a 5-year period, while it decreased by 10% with damp. Over the same time span, increased damp caused a slower rate of deterioration in hydraulic conductivity and thermal insulation [26]. Pratiwi et al. [27] studied the capillary rise levels of heritage structures in Jakarta's Kota Tua neighborhood, focusing on the Cipta Niaga structure. These architectural masterpieces are seriously threatened by capillary rise, which increases the wall moisture content and causes structural degradation. Gravimetrics was used by the researchers to measure the capillarity-related damage. According to the study, the capillary water concentrations of some wall portions were greater than the hygroscopic water content. This highlights the importance of considering capillary growth when preserving historic structures [27]. Goudjil et al. examined a novel polarization-based removal method in an effort to eliminate the need for release agents and lessen the hazards that accompany them for both the environment and consumers. Experiments were conducted at 20 ± 2 °C on regular concrete C25/30 to assess how the approach in producing a smooth concrete surface and a successful demold. The study outlines the best practices and techniques to obtain acceptable demolding outcomes without the use of conventional release agents [28].

The capillary water absorption characteristics of natural construction stones have been the subject of numerous studies. Capillary water absorption is one of the greatest indicators of water permeability in natural stone [29]. Many natural stones lose their mechanical and physical qualities as a result of water absorption from capillaries and excessive porosity. In cold temperatures, water that is absorbed through capillary action freezes and transforms into ice. Pressure builds up in the pores as a result of the ice crystals' development and volume expansion, greatly reducing the strength of the rock. This also applies to salts that crystallize when water seeps through natural stones [30]. Washburn was the first to study capillary water flow kinetics in porous media mathematically. Tomašić et al. used two distinct varieties of limestone to test the capillary water absorption in turbulent waters and found that the structural characteristics of the stone can influence capillary water absorption [30]. Three distinct granite types' capillary water absorption capacities ranged from 0.24 to 1.24 $kg/m^2\ s^{0.5}$, according to research by Mosquera et al. [31].

The study conducted by Rirsch and Zhang examines the impact of the mortar properties and water absorption on the occurrence of rising damp, a phenomenon that leads to the deterioration of structures due to moisture and salt accumulation. The study presents findings from a one-year experiment that quantified the vertical increase in dampness on walls constructed using various mortars and subsequently contrasted these measurements with theoretical forecasts. The study demonstrates that the Sharp Front Model accurately characterizes the phenomenon of rising damp and that the key factor influencing the height of the damp front is the rate of water absorption. Furthermore, it suggests that addressing rising damp can improve the thermal efficiency of walls by decreasing evaporation [32]. The transmission of liquid water in porous building materials and its hygrothermal impact were investigated by Lu et al. [33]. The authors highlighted the importance of the capillary water absorption coefficient in accurately simulating moisture transfer. They also suggested an enhanced continuous measuring technique to address the constraints of the conventional method. The authors conducted a comparative analysis of the outcomes acquired from conventional and continuous approaches, utilizing autoclave concrete that was aerated as a case study. The authors emphasized the enhanced precision, ease of use, and replicability of the latter option. The research highlights the importance of employing accurate mea-

surement procedures and proposes the utilization of more dependable methodologies for future investigations in this particular domain [33]. The study undertaken by Çelik and Sert aimed to examine the influence of water absorption and the crystallization of salt on the long-term resilience of Döğer tuff, a frequently employed construction material in cultural heritage locations within Turkey. The research encompassed a comprehensive analysis of the chemical, mineralogical, petrographical, and physicomechanical properties in order to investigate the degradation characteristics of the material when exposed to different salt solutions and concentrations. The results indicate that the utilization of Döğer tuff in the construction of structures may give rise to durability concerns due to the significant absorption of capillary water and subsequent deterioration of physical and mechanical characteristics. The examination of moisture transfer within the walls of buildings holds significant importance in understanding the behavior associated with durability and the deterioration of their appearance. The significance of moisture transport via building walls in evaluating durability and maintaining visual appeal is understood. An examination of moisture and heat movement in historic walls is necessary to address the problem of increasing humidity. Several computing programs, which have been examined in this study under various boundary conditions, enable the execution of such analyses [34].

According to Çelik and Köken [35], the process of capillary water absorption is mostly influenced by the size and shape of the pores. In their work, Çelik and Yılmaz [36] investigated the impact of capillary water on the process of weathering in natural construction stones. The study specifically examined the mineral deposits of andesite, Ayazini, and Seydiler in Afyonkarahisar. The attributes of the stones were characterized by the researchers, encompassing their petrographic–mineralogical traits, their chemical compositions, the distribution of pore sizes, and the physicomechanical characteristics. The study conducted experiments to assess the process of water absorption under static, saline, and acidic conditions. The absorption rates of andesite, Ayazini tuff, and Seydiler tuff ranged from 5.83 to 6.88 $kg/m^2\ s^{0.5}$, 21.18 to 22.46 $kg/m^2\ s^{0.5}$, and 7.05 to 9.30 $kg/m^2\ s^{0.5}$, respectively. The pH value of 3 exhibited the greatest absorption rate. The findings emphasize the variations in the capillary water absorption capacity across various stone types, which is crucial in evaluating the long-lasting nature of construction [36]. The study conducted by Karagiannis et al. examined the phenomenon of capillary absorption in building materials, a critical aspect in comprehending their long-term endurance and service life. A first-order mathematical model was constructed to elucidate the process of capillary water uptake in the presence of dynamic environmental variables. Subsequently, this model was verified through a comparison with experimental data. The findings suggest that the absorption characteristics are affected by both the features of the material and the surrounding conditions. The incorporation of environmental data leads to enhanced accuracy, as evidenced by a comparison with a comparable model. The model demonstrates a high level of accuracy in forecasting water absorption during severe weather conditions, rendering it valuable for the development of simulators and tools for risk evaluation aimed at addressing climate change-related issues [37].

The literature review indicates that international research has not extensively and systematically addressed the issue of masonry dehumidification. This is evident from the significant disparity between the number of international journal papers [14] dedicated to studying the mechanisms, effects, and measurement of rising damp in building materials and the papers focused on strategies for its removal.

Some authors argue that experimental investigations are excessively costly and time-consuming [38]. Consequently, researchers have developed calculative methods to model the behavior of moisture in building materials. One such method is WUFI 2D, which simulates heat and moisture transfer [39]. After careful consideration, numerical simulations have certain limitations with regard to accurately simulating the rising damp phenomenon in actual historical walls. Therefore, we cannot solely rely on them to investigate repair options. Experimental investigation continues to be the predominant method employed to study anti-dampness treatments, and it can be conducted at several levels.

Some research studies utilize laboratory-scale masonry models that vary in terms of size and form. The structures of small-scale masonries present inherent complexities, and the replication of rising damp in laboratory settings poses significant challenges, mostly because of the inherent difficulty in producing mortars with adequate sorptive properties [1]. In any scenario, the acquisition of data from actual structures can prove highly valuable, particularly when conducted through systematic surveys. This is exemplified by the case of Adelaide, South Australia, where the phenomenon known as salt damp, characterized by a combination of rising damp and a significantly elevated salt concentration, has resulted in the substantial deterioration of historical building materials. Consequently, this issue has necessitated extensive repair efforts employing various methodologies throughout previous decades [1].

The concepts of electro-osmosis have found technological uses in clay soils, such as humidifying dry soils or consolidating wet soils. In this situation, evidence of water flow and soil humidity changes has been reported [19]. Unfortunately, comparable experimental proofs do not exist regarding their applicability to construction materials [20]. Quantitative data on humidity changes following the deployment of dehumidification procedures, which are required for the proper evaluation of their actual efficiency, are limited in the technical literature [15].

The literature review shown above reveals the scarcity of research studies pertaining to the impact of electro-osmosis on masonry walls. Furthermore, there is a lack of field investigations of these systems in the existing literature [1]. In contrast, scholarly research has examined the ways in which building materials absorb moisture, leading to the establishment of moisture absorption coefficients. This work aimed to experimentally analyze the drying potential of the electro-osmosis technology for building elements and suggest the moisture repulsion coefficient, which was previously unstudied. Furthermore, upon reviewing the literature, it becomes evident that experimental investigations have been conducted on a laboratory scale. This study involved the implementation of a real-scale application, wherein measurements were collected and assessed over a long period of time.

This paper presents the findings of experiments conducted to investigate the elements that impact electro-osmosis in masonry, with the goal of determining its practical suitability for the removal of moisture from damp walls. In the present study, the objective was to investigate the long-term drying efficacy of capillary moisture repulsion apparatus utilizing the electro-osmosis technique. The Gül mosque was chosen as a representative historical structure affected by structural issues resulting from water absorption through capillary action within microchannels on its walls. The initial deployment of the device occurred on 24 January 2017, followed by a series of six measurements conducted at specific intervals until 2 August 2022. The moisture repulsion system maintains the dryness of building elements over the long term by establishing a natural barrier (potential barrier) between the building wall and the ground as water in the building foundation ascends into the structure via capillarity. This process takes approximately 277 days and occurs through channels where water molecules traverse. Building elements with high humidity are pushed to the ground for drying purposes. The research findings offer significant insights for professionals, researchers, and decision-makers in the construction industry.

2. Materials and Methods

2.1. Electro-Osmosis Device for Removal of Capillary Rising Damp

The process of moisture being absorbed and transferred in porous building materials is a multifaceted and intricate phenomenon that involves the interplay of several driving forces [40]. The soil contains a substantial quantity of water that has the ability to ascend the structure. Capillarity is the sole factor responsible for the upward movement of water, even in the presence of gravitational forces. The construction elements contain a vast network of interconnected capillary tubes, amounting to millions. The upward movement of water within the structure is facilitated by the presence of capillaries. The primary determinant of structural deterioration is the presence of salt molecules in the water. As

water molecules ascend the structure through capillary action, they transport the salts present in the soil. As the water ascends the building carriers and walls, it undergoes evaporation. Meanwhile, the salt is retained within the empty spaces in the concrete, creating a foundation for the ascent of fresh salty water as a result of the potential difference (Figure 1). The structure's walls permeate the wall in a way that is analogous to the manner in which moisture and salts accumulate water, resembling a sponge. A rise in moisture levels can be attributed to the direct interaction between the wall and the floor. While this is common for older structures, modern structures may experience a deficiency in interlocking as a result of structural flaws. The salts present in the soil undergo dissolution in water and then combine with it, resulting in their transportation into the wall alongside the water. Over time, the process of salt transport occurs within the wall, wherein it migrates towards the surface and then accumulates. The evaporation of moisture from the surface of the wall results in the formation of salt crystals. The accumulation of salt can lead to the chemical decomposition of plaster and masonry, potentially resulting in the destruction of the building structure. The optimal resolution to this issue is to refrain from cleaning and painting the expelled salt, as doing so will result in the salts within the wall resurfacing. Eliminating this particular form of dampness through structural techniques poses significant challenges. The prevention of dampness can only be achieved from one side by excavating and pitting the base, as well as by implementing or fixing a drain. By implementing these steps in conjunction with an electronic–physical drying process, the possibility of achieving a more favorable outcome is enhanced.

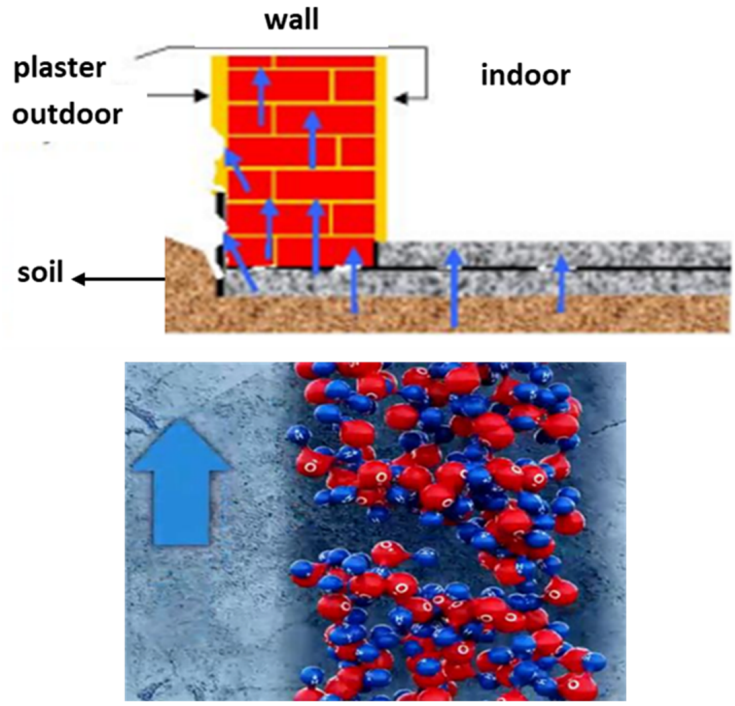

Figure 1. Water and salt molecules climbing a structure (The blue arrows indicate the presence of rising damp) [41].

Conversely, the corrosion of reinforcing steel resulting from elevated humidity levels within walls poses a significant concern in reinforced concrete structures, resulting in cost ramifications, substantial safety hazards, and adverse environmental consequences. Steel has inherent instability over its lifespan. It possesses the capacity to undergo oxidation and revert back to its initial state. When incorporated into concrete, it undergoes passivation due to the concrete's high alkalinity, rendering it resistant to corrosion. However, the water present in the soil transports the salt from the soil as it ascends the structure. The passive layer undergoes degradation upon the introduction of chloride and carbon dioxide. Various

salts, including carbon, magnesium, nitrate, and sulfate, have the potential to induce corrosion and impair the adhesion between concrete and steel. The process of steel corrosion refers to the degradation of steel due to chemical or electrochemical reactions. The volume of the corrosion product is greater than that of the steel. The aforementioned product induces mechanical strains that might lead to the occurrence of cracks and disintegration in concrete. The presence of salt water leads to a decrease in both the strength of steel and the strength of concrete when subjected to compressive forces. Additionally, the adhesion of the concrete deteriorates due to the formation of concrete corrosion (Figure 2).

Figure 2. The product resulting from the corrosion of steel in a structure and damage to concrete [41].

The functionality of the capillary moisture-repellent device can be observed subsequent to its initial setup. The technology employs the principle of electro-osmosis to resist groundwater that attempts to ascend the building. Once the damage has been accurately diagnosed and the measuring sites have been determined, the capillary moisture repellent is applied. The wall is equipped with many adaptable electrodes. The capillary moisture repulsion device control unit connects these electrodes to a reference electrode, which is either buried in the ground or connected to the earthing line in the current electrical system. The operational mechanism of the construction involves the application of an external electrical voltage to facilitate active desalination and dehumidification. The capillary moisture repulsion device is responsible for generating electric potentials that regulate the movement of salt and inhibit the movement of capillary fluids in the process known as electro-osmosis. Regular measurements are conducted to assess the moisture content of the walls. It is anticipated that the capillary moisture repellent will establish an uninterrupted barrier, thereby impeding the re-entry of moisture. Following the successful processes of dehumidification and desalination, it is imperative that the capillary moisture repellent remains within the structure and sustains its operational effectiveness. The presence of a potential barrier, which acts as a natural barrier between the wall and the floor, facilitates the moisture repellent's ability to maintain dryness on the walls. The objective of the system is to effectively remove moisture and salt molecules from the structure, extending them

beyond the foundation, in a manner consistent with their initial entry point, without the need for any construction activities such as plastering and painting. Capillary moisture repulsion devices facilitate the alignment of the load exerted by the building walls with the mineral water present in the soil. The graphic representations in Figure 3 depict the device and the electrodes that are strategically placed on the walls.

Figure 3. First stage of installation of the capillary moisture treatment device [41].

During the process of moisture removal from walls, water tends to seek the shortest route out. Particularly in cases in which the walls are wide, the surface evaporation can exceed the overall water accumulation. Effective and appropriate ventilation enhances the rate of evaporation, hence expediting the drying process of the wall. The presence of blisters may indicate the occurrence of water flow and evaporation. Regularly cleaning blisters can yield insights about the movement and evaporation of water from the wall. The utilization of measuring rods for wall depth measurement typically yields a maximum wall depth measurement of 100 mm. Consequently, all measurements will be conducted at the location with the highest concentration of infiltrating water. The aforementioned measurements hold significance in comprehending the dynamics and dispersion of water within the wall. In order to ensure the efficient management of the removal process, it is imperative to conduct regular measurements and closely monitor indicators such as heaving. The monitoring of the removal process and the implementation of appropriate measures are crucial for the long-term maintenance of building health. The visualizations depicted in Figure 4 illustrate the movement of water molecules (blue arrows in Figure 4) as they exit the building and then return to the ground subsequent to the implementation of a capillary moisture-repellent device (The device is shown in the red circle in Figure 4). The device's characteristics are provided in Table 1.

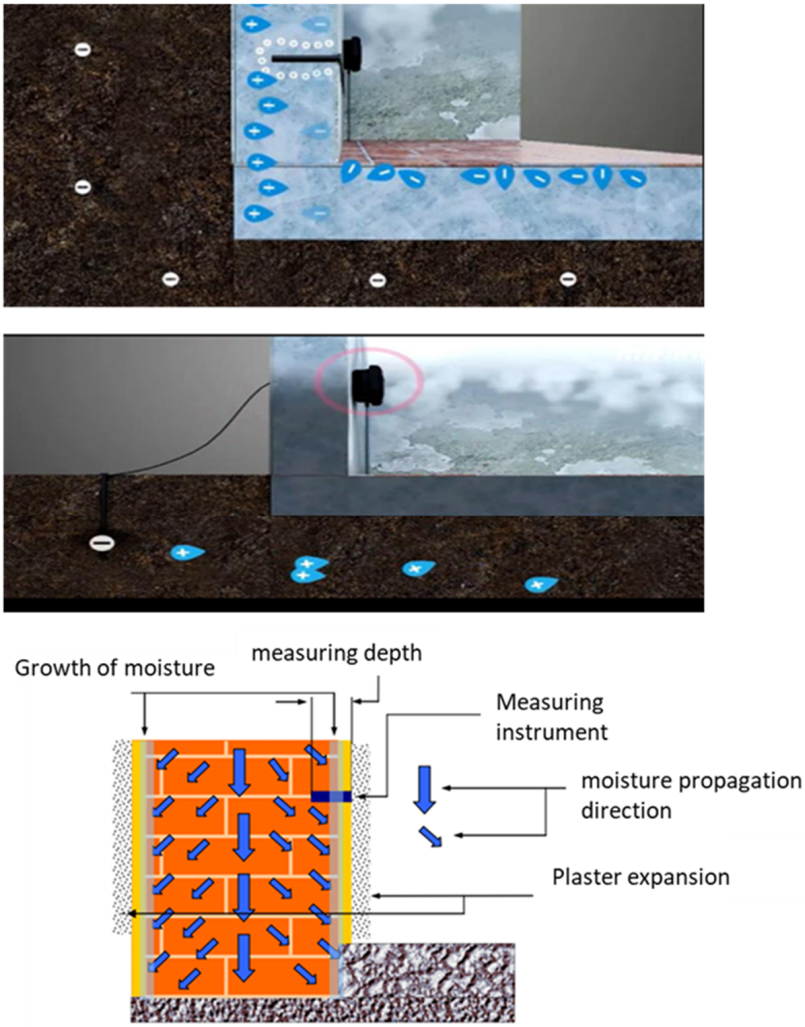

Figure 4. Treatment of rising damp [41].

Table 1. Characteristics of the device.

Brand	**Mirline ©**
External body material	Polypropylene
Dimensions	W × H × D = 342 × 194 × 135 mm
Mass	2.8 kg
Connection	220 V 50/60 Hz
Consumption	11 W
Signal frequency	141 kHz
Ferrit antenna frequency	141 kHz
Dry electrode electric current supply	0.7–2.0 V
Frequency band	f: 0.14–0.826 MHz
Effective value of electric reserve field strength	333.3 V/m
Magnetic backup field effective value of intensity	2.35/f A/m
Potential equalization rod for ground	Dimensions: 16 × 10 × 1000 mm, Current: 16A/5
Cable between device, electrodes, and ferrite antenna	Coaxial cable type RG58

2.2. Implementation of System

The Gül mosque in Istanbul, Turkey was subjected to the application of the system. The construction date of the structure is uncertain; nevertheless, it was once a Byzantine church. Following the conquest, it underwent transformation into shipyard storage for a period of time, before being repurposed as a mosque [42].

The mosque exhibits clear indications of Byzantine and Ottoman architectural influences. The outside architecture of this church underwent many modifications during the

Turkish period. The two bilateral facades were constructed with numerous windows, and their ridge line was progressively capped, resembling the architectural style observed in several Ottoman mosques. A Turkish building is characterized by the presence of very flattened, octagonal domes that are devoid of sound and equipped with octagonal pulleys. Hence, it is evident that the ancient church underwent renovations in accordance with the classical era of Turkish architecture, encompassing the side facades, the substantial supporting arches, and the central dome. The church, initially characterized by its impressive proportions due to its elevated basement, likely achieved an even more impressive visual impact with its dome, which would have been supported by a tall pulley. The minaret of the mosque bears a resemblance to the minarets constructed in the aftermath of the 1766 earthquake, including a baroque profiled balcony design [42].

The Gül mosque was built on a brick vaulted basement. The mosque is situated on an elevated site. The building sits on gravel, sand, clay, and silt soil (sedimentary soil). The building content of the mosque shows an alternating style comprising faceted stone and classical brickwork, with Khorasan joints. Stone and brick have been mixed into the masonry (Figure 5). The mosque has a total exterior wall area of 1560 m^2. It has a total external wall volume of 312 m^3. Due to its proximity to the sea, the mosque has long been plagued by moisture and dampness issues caused by the ground (Figures 6 and 7).

Figure 5. Gül mosque.

The capillary moisture-repellent device was strategically positioned within the mosque, specifically in the designated area denoted as (2) in the provided layout plan depicted in Figure 8. The device was positioned at a vertical elevation of approximately 2.5 m above ground level, as illustrated in Figure 9. The device's location was determined based on the coverage areas and availability of electricity. Given that the device produces a circular impact, center points were chosen to maximize the effect. Furthermore, due to the building's historical significance, a site was carefully selected to ensure a minimal impact on its historical integrity.

Figure 6. General view inside the mosque.

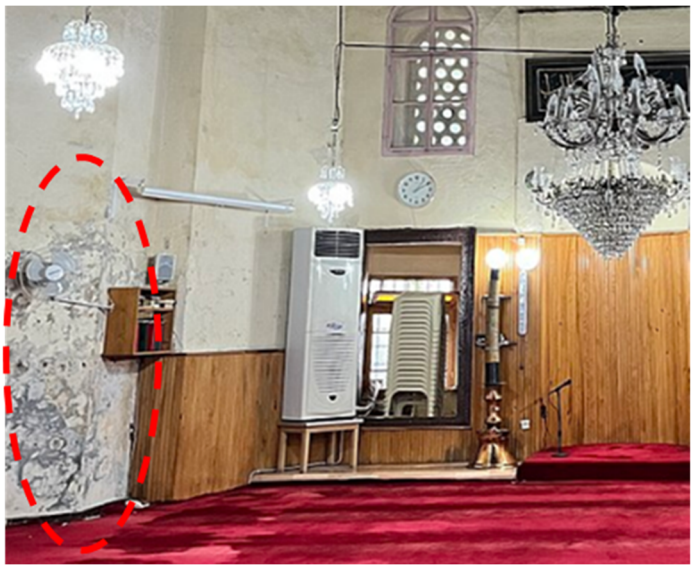

Figure 7. Persistent issue of dampness and humidity within the mosque.

The system's electrodes were affixed to the walls at the four designated locations indicated by (1) in the layout plan (Figure 8). The electrodes were positioned at a height of 290 cm from the ground (Figure 10). Given that the device was positioned at the center of the circle, electrodes were placed at four diametrically opposite points, with the device located in the middle. Thus, the circular effect was transformed into a spherical one, facilitating more rapid moisture removal. Furthermore, the structure is constructed using masonry stone and is completely interconnected throughout, without any gaps present. As a consequence, load-bearing elements and exterior walls were outfitted with electrodes in order to guarantee that the electrical signal transmitted by the electrodes could entirely affect the structure.

Figure 8. System layout.

Figure 9. Installation of the capillary rising damp treatment device.

Subsequently, measuring points were carefully placed at 8 distinct locations (3.1–3.8) to quantify the water content within the walls. Measurements were obtained at three distinct heights at each measurement point: 50 cm at the bottom, 120 cm at the middle, and 200 cm at the top. The inserted measuring rods are capable of measuring at a maximum wall depth of 100 mm, specifically targeting the area where the largest amount of water penetration occurs. Measurements were taken at a depth of 90 mm in this study. A total of 24 measurements were collected in each measurement period. The Gann Hydromette device was utilized to collect measurements from the designated measurement locations. Subsequently, the Gann values were employed to determine the weight and volume of water present in the material [43]. Following the initial implementation of the device (t_0), a series of five subsequent measurements were conducted on distinct dates (t_1–t_6), and the outcomes were then assessed.

Figure 10. Electrode mounted on the vertical axis (shown in a red circle).

2.3. Evaluation of Measured Results

The capillary water absorption coefficient is commonly employed in practical engineering to assess the liquid water transmission capability of building components. This coefficient can be determined using Equation (1) [44]. The literature utilizes the EN 1925 [45] standard to establish the levels of capillary water absorption. The capillary water absorption coefficient is then calculated using the method provided in Equation (1). Given the physical similarity between the capillary water repulsion mechanism and capillary water absorption, this study utilizes the expression specified in Equation (1) as the capillary water repulsion coefficient (C) to assess the effectiveness of the capillary rising damp treatment system. This equation was used to assess the process of capillary water repulsion in the system.

$$C = \frac{\Delta M}{A_c \times \sqrt{t}} \quad (1)$$

The expression $\Delta M = M_i - M_s$ (kg) represents the total mass of water repulsion on the wall. It is calculated by subtracting the weight of the wall before water repulsion (M_i) from the weight of the dried wall (M_s). A_c represents the cross-sectional area of the wall in contact with water (m^2), and t denotes the time at which the measurements were taken. Another factor to consider is the mass reduction. The aforementioned statement is formally defined as the ratio of the overall decrease in mass divided by the cross-sectional area that is in direct contact with water.

$$\Delta M'' = \frac{\Delta M}{A_c} \quad (2)$$

In the calculations, the wall depth (w) is determined to be 0.55 m, the overall length of the wall (L) is 120 m, the cross-sectional area of the wall (A_c) is 66 m^2, and the material density is 2300 kg/m^3.

3. Results and Discussion

This section presents an evaluation of the measurement results acquired using the aforementioned procedure. A total of 24 Gann Digit measurement results were assessed at eight distinct horizontal locations and three distinct vertical points during each measurement step. The tables and graphs presented below depict the use of a singular Gann Digit value, which serves as the mean value for each measurement time (t). Tables 2 and 3 present additional variables derived from the average Gann Digit measurement data.

In order to determine the weight percentage of water in all walls of the building, the mass of water per unit building volume, and the overall water content, the Gann Digit values obtained from the moisture measurement device were calculated using the appropriate conversion chart [45]. The aforementioned calculations were repeated for each

time step, and the results are presented in Table 2. The reduction in mass represented in the table was determined by calculating the difference in the total mass of water within the structure during the two measurement intervals. To determine the unit mass reduction, the total mass reduction was divided by the cross-sectional area (A_c) perpendicular to the direction of capillary water movement throughout the walls.

Table 2. Measurement results.

Measurement Step and Date	Gann Digit Value	Moisture Content by Weight (%)	Unit Water Mass (kg/m^3)	Total Water Mass M (kg)	Mass Reduction ΔM (kg)	Unit Mass Reduction ΔM″ (kg/m^2)
t_0 (24 January 2017)	88.24	14.48	333.0	103,896	-	-
t_1 (7 June 2017)	78.81	5.20	119.7	37,346	66,550	1008
t_2 (28 October 2017)	72.50	3.75	86.3	26,926	10,421	157.9
t_3 (25 March 2018)	68.30	3.28	75.3	23,494	3432	52.0
t_4 (24 September 2018)	65.20	3.02	69.4	21,653	1841	27.9
t_5 (20 March 2019)	63.10	2.94	67.5	21,060	593	8.9
t_6 (2 August 2022)	61.85	2.90	66.6	20,779	281	4.2

Table 3 presents the capillary moisture repulsion coefficients, which were derived by taking into account the time interval between the reference measurement point (t_0) and subsequent measurement intervals ($t_{1–6}$). For instance, during the reference period t_0–t_6, there was a time span of 2016 days between the two measurement sites. During this period, the total drop in water mass amounted to 83,117 kg, whereas the reduction in unit mass was 1259 kg/m^2. The capillary moisture repulsion coefficients were computed for various time factors (second, hour, day) throughout the measurement period t_0–t_6, based on the provided values.

Table 3. Calculations derived from the initial reference value.

Variables		Measurement Period					
		t_0–t_1	**t_0–t_2**	**t_0–t_3**	**t_0–t_4**	**t_0–t_5**	**t_0–t_6**
Mass Reduction (ΔM)	kg	66,550	76,970	80,402	82,243	82,836	83,117
Cross-Sectional Area (A_c)	m^2	66	66	66	66	66	66
Unit Mass Reduction (ΔM″)	kg/m^2	1008	1166	1218	1246	1255	1259
Interval between Measurements (t)	Days	134	277	425	608	785	2016
	Hours (h)	3216	6648	10,200	14,592	18,840	48,384
	Seconds (s)	11,577,600	23,932,800	36,720,000	52,531,200	67,824,000	174,182,400
Time Factor ($t^{0.5}$)	$s^{0.5}$	3403	4892	6060	7248	8236	13,198
	$h^{0.5}$	56.7	81.5	101.0	120.8	137.3	220.0
	$day^{0.5}$	11.6	16.6	20.6	24.7	28.0	44.9
Capillary Moisture Repulsion Coefficients (C)	kg/m^2 $s^{0.5}$	0.296	0.238	0.201	0.172	0.152	0.095
	kg/m^2 $h^{0.5}$	17.78	14.30	12.06	10.32	9.14	5.73
	kg/m^2 $day^{0.5}$	87.11	70.07	59.09	50.54	44.80	28.05

The calculation of the capillary moisture repulsion coefficients in Table 4 was based on the periods observed at consecutive measurement points and the measurement results obtained between these points, rather than considering the periods between the reference measurement point (t_0) and subsequent measurement times.

Table 4. Computations derived from consecutive measurement data points.

Variables		Measurement Period					
		t_0–t_1	t_1–t_2	t_2–t_3	t_3–t_4	t_4–t_5	t_5–t_6
Mass Reduction (ΔM)	kg	66,550	10,421	3432	1841	593	281
Cross-Sectional Area (A_c)	m^2	66	66	66	66	66	66
Unit Mass Reduction ($\Delta M''$)	kg/m^2	1008	157.9	52.0	27.9	8.9	4.2
Interval between Measurements (t)	Days	134	143	148	183	177	1231
	Hours (h)	3216	3432	3552	4392	4248	29,544
	Seconds (s)	11,577,600	12,355,200	12,787,200	15,811,200	15,292,800	106,358,400
Time Factor ($t^{0.5}$)	$s^{0.5}$	3403	3515.0	3575.9	3976.3	3910.6	10,313.0
	$h^{0.5}$	56.7	58.6	59.6	66.3	65.2	171.9
	$day^{0.5}$	11.6	12.0	12.2	13.5	13.3	35.1
Capillary Moisture Repulsion Coefficients (C)	$kg/m^2\ s^{0.5}$	0.296	0.04	0.01	0.007	0.002	0.0004
	$kg/m^2\ h^{0.5}$	17.78	2.70	0.87	0.42	0.14	0.02
	$kg/m^2\ day^{0.5}$	87.11	13.20	4.27	2.06	0.68	0.12

Figure 11 presents the results of Table 3, illustrating the computed capillary moisture repulsion coefficients between the reference measurement point (t_0) and other measurement intervals ($t_{1–6}$). The results demonstrate a linear decrease in the capillary moisture repulsion coefficient with time following the implementation of the device, as compared to the reference period. The cause of the linear decline in the results can be elucidated as follows: the water repellency of the material is determined by both the total water content and the amount of water that is repelled within a specific timeframe. At the start, when the body contains the largest amount of water and is almost saturated, the potential difference between the soil and the wall is at its highest. Thus, the first measurement period yielded the greatest amount of water propelled per unit time and the highest moisture repulsion coefficient. Based on Equation (1), the capillary moisture repulsion coefficient states that the water repulsion coefficient of a surface in contact with water is inversely proportional to the square root of time. Upon the examination of the experimental studies in the literature, it was found that the water absorption coefficient also exhibits a linear change, which can be attributed to a similar physical mechanism [36]. The value of C drops from 0.296 $kg/m^2\ s^{0.5}$ during the measurement period t_0–t_1 to 0.095 $kg/m^2\ s^{0.5}$ when the measurement period t_0–t_6 is considered as the reference. Hence, it is crucial to consider the reference time period when determining the capillary moisture repulsion coefficient.

The capillary moisture repulsion coefficients obtained within the time interval between the two measurement periods are depicted in Figure 12. In the measurement period t_0–t_1, the value of C was recorded as 0.296 $kg/m^2\ s^{0.5}$. However, during the subsequent measurement period t_5–t_6, this value underwent a substantial decrease of about 99% and was calculated as C = 0.0004 $kg/m^2\ s^{0.5}$. The building substrate was almost completely saturated with water prior to the installation of the system. Upon the activation of the system, the drying process started. Throughout the calculation of the moisture repulsion coefficient, measurements were taken at eight horizontal locations. At each location, measurements were obtained at three different heights: 50 cm at the bottom, 120 cm at the middle, and 200 cm at the top. The mass water ratio in the wall was determined by calculating the average of the 24 measurement points. The device primarily generates a pushing force near the height where the electrodes are positioned, but, over time, this force spreads towards the lower points of the wall. Therefore, the data indicate that the upper sections of the wall experience faster drying, while noticeable changes in the water mass fraction only occur in the lower part after a certain period of drying. In this context, although the time duration at $t_{5–6}$ was longer than the first measurement period, the C value obtained during the first measurement period was significantly higher than in the last period.

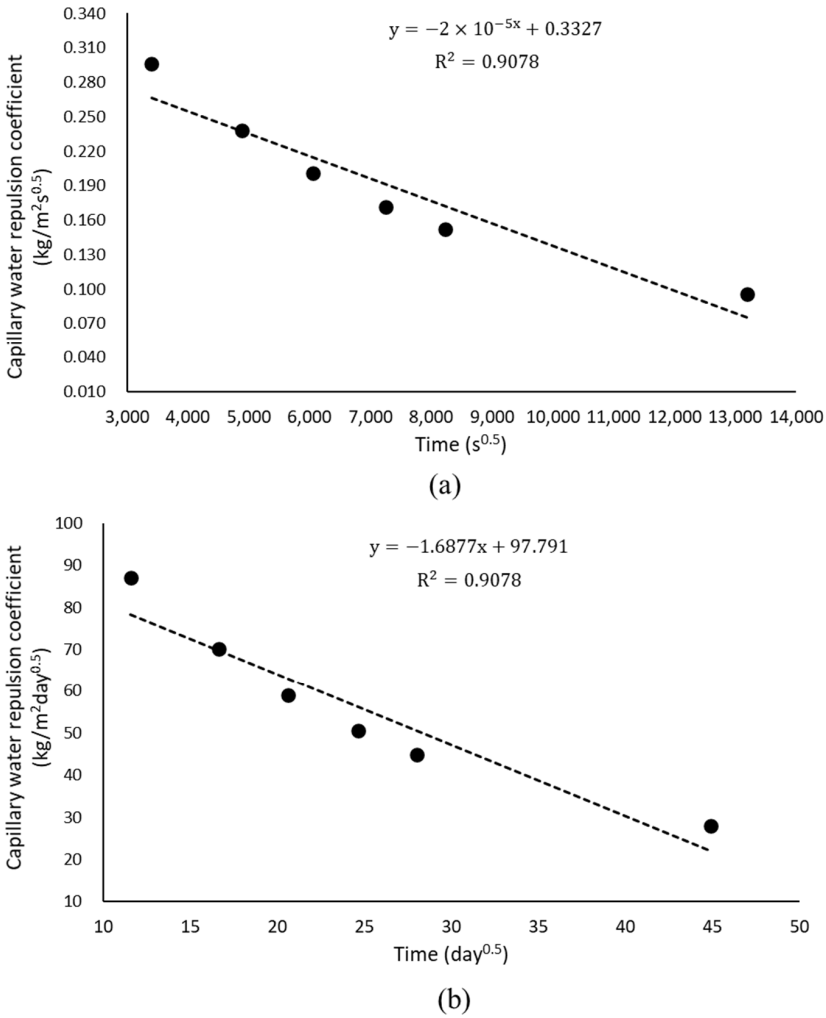

Figure 11. Capillary moisture repulsion coefficients obtained according to different time factors (**a**) The time scale is a second, (**b**) The time scale is a day.

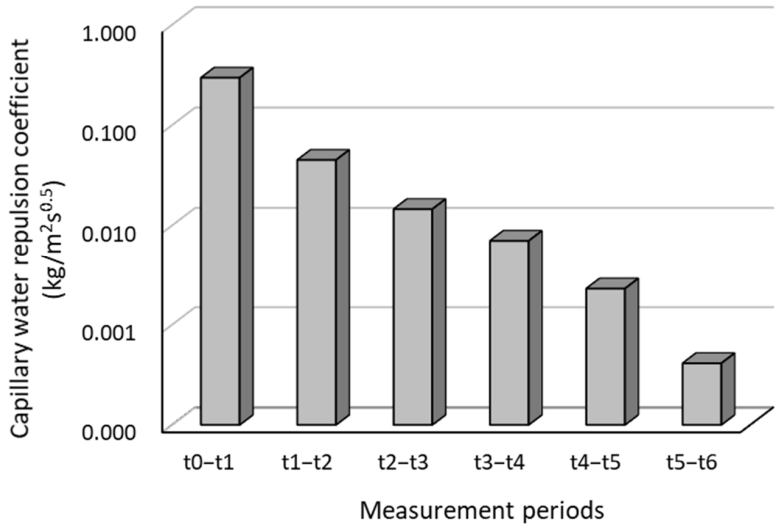

Figure 12. Variations in capillary moisture repulsion coefficients at each measurement interval.

Figures 13 and 14 display the results of the time-varying fraction of water mass in the masonry walls. The results demonstrate that when the capillary moisture repulsion apparatus is activated, it effectively expels moisture from the building structure by directing

it through the pre-existing capillary channels and into the soil. However, as the amount of water in the structure decreases over time, the rate of moisture removal also diminishes. The presence of a logarithmic decline in the water mass ratio over time was established with a coefficient of determination (R^2) of 0.96. Initially, the water content in the structure was 14.48% (classified as very wet). However, over time, it decreased to 5.2% on the 134th day (t_1). Eventually, it dropped below the crucial dryness threshold of 4% and reached 3.75% on the 277th day (t_2) at the measurement time. The moisture pushing mechanism effectively reduced the moisture content in the masonry walls from a 'very wet' level to a 'dry' level during a period of approximately 9 months. After reaching a critical point, the mass of water remained relatively stable. At the third measurement point (t_3), the water content decreased to 3.28%. At the fourth measurement point (t_4), the water content decreased further to 3.02%. At the fifth measurement point (t_5), the water content decreased to 2.94%. Finally, at the sixth measurement point (t_6), the water content decreased to 2.90%. Despite the 1231-day duration between the measurement intervals (t_5–t_6), the mass fraction of water in the structure only changed by 0.04% during this period.

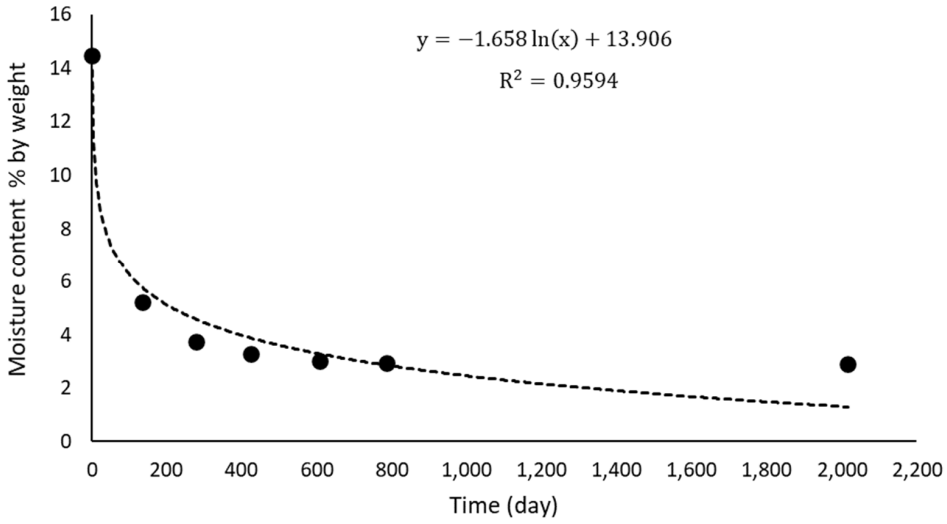

Figure 13. Time-dependent variations in the mass fraction of water in the masonry walls.

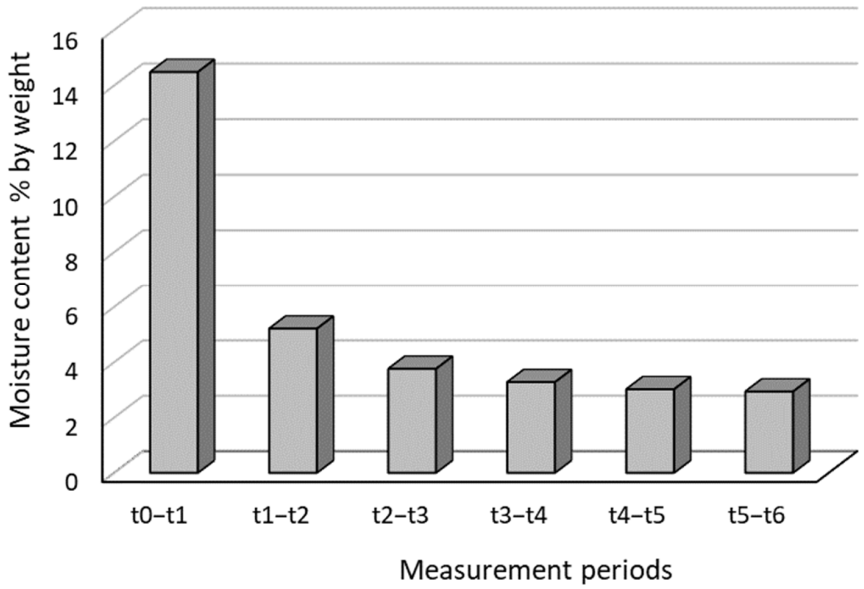

Figure 14. Variations in the mass fraction of water within the masonry wall during different measurement intervals.

The referenced literature [46] determines the water absorption coefficient by subjecting samples of specific dimensions to controlled water absorption and measuring the amount of water that they absorb over time. The water absorption coefficient of the material is calculated by measuring the time (t) at which the water absorption reaches a steady level and the associated rise in mass. In this study, the same approach was employed, but a reduction in mass rather than an increase in mass was investigated. In this regard, fluctuations in the water mass fraction within the masonry wall throughout different measurement intervals were investigated.

Upon analyzing the time variation graphs (Figure 15) of the decrease in water mass per unit area due to capillary thrust and the ratio of water pushed to the dry mass, it is evident that the majority of water in the structure is displaced over the time period $t_{0–1}$. Over the period of 134 days, a significant amount of water, specifically 66,550 kg out of a total of 103,896 kg, was displaced from the structure and absorbed into the ground. During the remaining 1882 days in the $t_{5–6}$ period, a total of 16,617 kg of water was released into the soil. Moreover, the capillary repulsion for each unit cross-sectional area was as follows: $\Delta M'' = 1008\ kg/m^2$ in the period $t_{0–1}$, 157.9 kg/m^2 at $t_{1–2}$, 52 kg/m^2 at $t_{2–3}$, 27.9 kg/m^2 at $t_{3–4}$, 8.9 kg/m^2 at $t_{4–5}$, and 4.2 kg/m^2 at $t_{5–6}$. Despite the greater duration of time at $t_{5–6}$ compared to the other measurement periods, there was minimal change in the capillary repulsion value in comparison to the preceding period. Thus, the measurement point (t_5), at which the capillary repulsion remained almost constant, was utilized to ascertain the final capillary moisture repulsion coefficient. This can be explained by the fact that, during the $t_{5–6}$ period, the wall's dryness resulted in a reduction in the amount of water that was extracted. Furthermore, as a result of the walls drying out, there was a greater possibility of water being drawn up through capillary action from the soil. Following this timeframe, the phenomenon of electro-osmosis acted as a deterrent to the upward movement of water, rather than causing the water to be pushed downward. When the unit time is measured in seconds (Figure 15a), the coefficient of capillary water repulsion is 0.152 $kg/m^2\ s^{0.5}$. However, when the unit time is measured in days (Figure 15b), this value is estimated at 44.8 $kg/m^2\ day^{0.5}$.

Figure 16 illustrates the relationship between the capillary water repulsion coefficient and the mass fraction of the water in the wall. Upon evaluating the acquired findings, it is established that there is a strong linear relationship between the change in the capillary moisture repulsion coefficient and the mass fraction of the water in the wall structure. This relationship is highly defined, with an R^2 value of 0.99.

Based on the literature research, an increase in the water content within the building elements leads to higher heat conduction coefficients and hence increases the heat loss. A study conducted under California's climatic conditions revealed that damp walls lead to a 19% increase in energy consumption during the months of December and January, compared to dry walls. Conversely, the presence of water in the walls reduces the demand for cooling by up to 18% during the summer [47].

The presence of water within building materials' pores negatively affects their thermal insulation performance: a 1 wt% increase in moisture content is estimated to cause an increase of up to 5% in the thermal conductivity of masonry [21]. Hence, porous bricks and stones may experience an increase of up to 100% in thermal conductivity due to saturation. Such unsuitable thermal transmittance of the damp envelope implies large energy consumption for the heating of historical buildings and a large environmental impact [14]. In the course of this investigation, the water mass fraction in the building was initially 14.48% before the system was built. However, in the most recent measurement, the value was reduced to 2.90%. Based on the given reference study, it can be inferred that the conduction heat transfer coefficient on the walls reduces by around 58% in this scenario. Therefore, it may be inferred that the heat losses from the walls have been substantially reduced, and this ratio is useful from an energy efficiency perspective in the construction project management field.

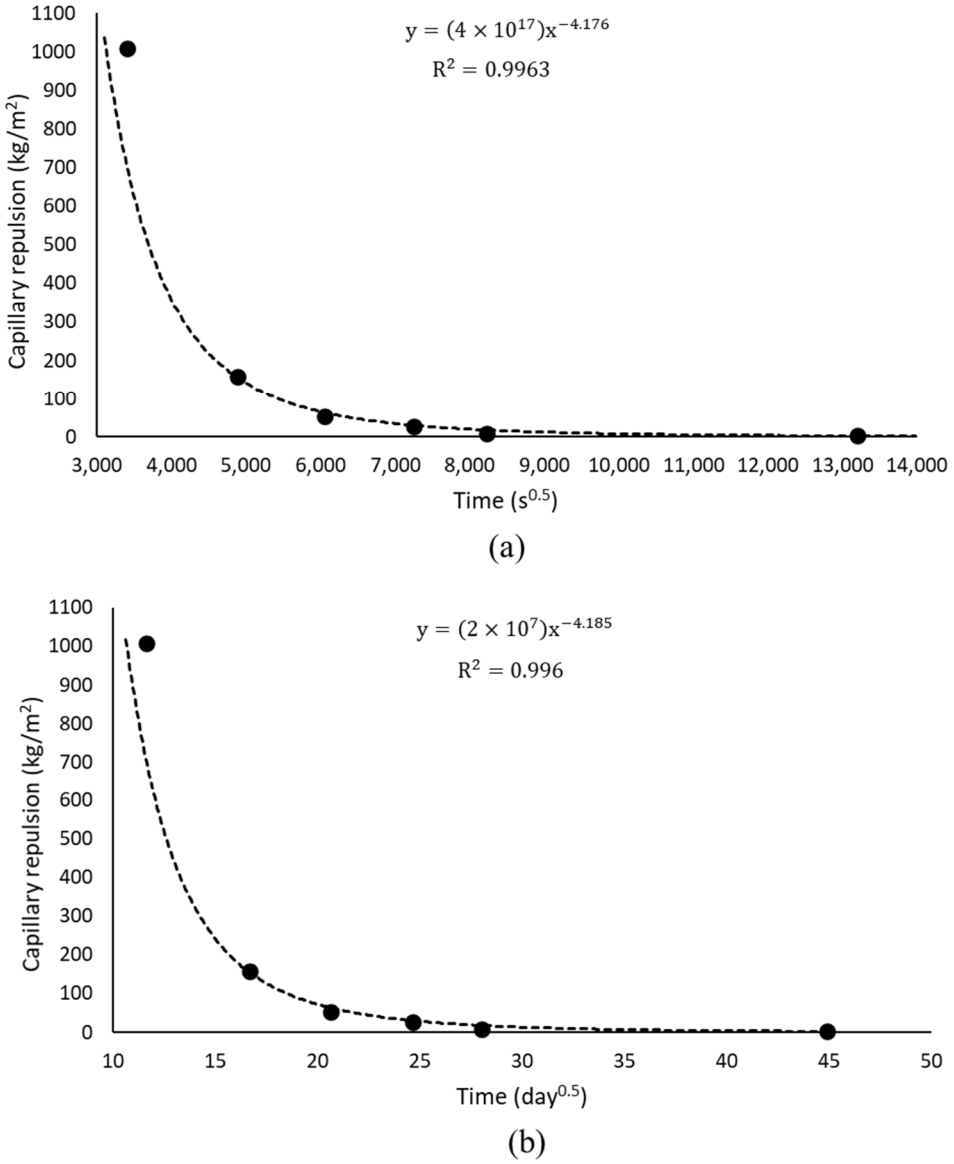

Figure 15. Moisture repulsion performance over time.

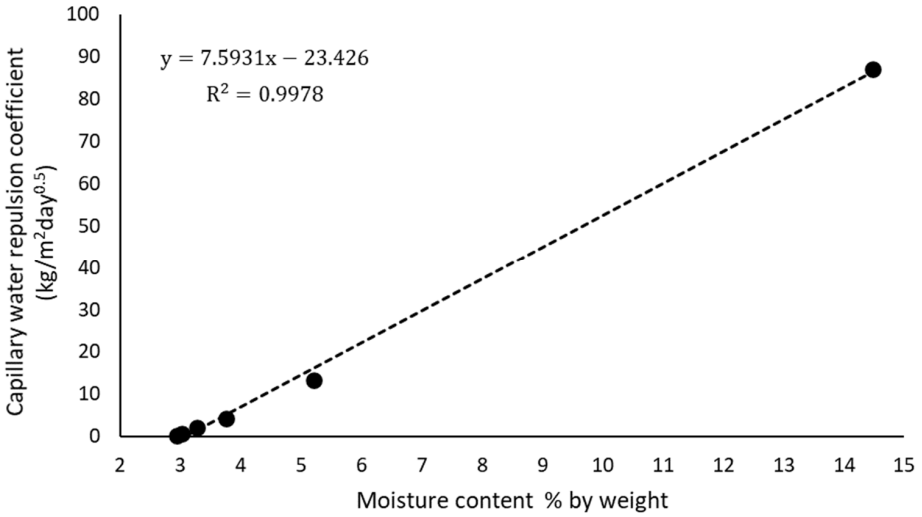

Figure 16. Variations in capillary water repulsion coefficient with mass fraction of water.

4. Conclusions

This study examined the long-term drying effectiveness of a capillary moisture repulsion system that utilizes electro-osmosis technology. The investigation focused on the Gül mosque, which experiences structural issues due to water absorption by capillary action on its walls. The initial installation of the device occurred on 24 January 2017, and a total of six measurements were conducted at specific intervals until 2 August 2022. A total of 24 measurements were collected, both horizontally and vertically. These measurements yielded the weight (%) of water in all walls of the building, the mass of water in the unit building volume, and the total amount of water. The acquired findings can be summarized as follows.

The presence of a logarithmic decrease in the water mass fraction over time was established at the $R^2 = 0.96$ level of precision. The initial water content in the structure was 14.48% (very wet) at t_0. However, this value was lowered to 5.2% at t_1 (134th day) and fell below the crucial dryness threshold of 4% (specifically 3.75%) at t_2 (277th day). The moisture repulsion mechanism effectively reduced the moisture content in the walls from a 'very wet' level to a 'dry' level within a timeframe of approximately 9 months. Following this critical point in time, the water mass exhibited minimal alteration. From this perspective, it is evident that the system not only transfers water from the wall to the soil; it prevents the uptake of water by capillary action by protecting the construction components that come into contact with damp soil.

After the device is installed, the capillary water repulsion coefficient falls in a linear manner over time, following the reference period. During the measurement period t_0–t_1, the value of C is 0.296 $kg/m^2\ s^{0.5}$. However, when the measurement period t_0–t_6 is used as a reference, the value of C reduces to 0.095 $kg/m^2\ s^{0.5}$.

During the measurement period from t_0 to t_1, the value of C was $kg/m^2\ s^{0.5}$. However, in the measurement period from t_5 to t_6, this value dropped by roughly 99% and was computed as 0.0004 $kg/m^2\ s^{0.5}$.

It was concluded that the majority of the water in the building was displaced over the time period from t_0 to t_1. Over the course of 134 days, a total of 66,550 kg of water, out of the initial 103,896 kg, was displaced into the soil. During the remaining 1882 days of the $t_{5–6}$ period, a total of 16,617 kg of water was displaced into the soil.

The final water repulsion coefficient was determined by using the measurement point (t_5) where the water repulsion remained almost constant. When the unit time is measured in seconds, the coefficient of capillary water repulsion is 0.152 $kg/m^2\ s^{0.5}$. However, when the unit time is measured in days, this value is estimated as 44.8 $kg/m^2\ day^{0.5}$.

After the installation of the equipment, the water mass ratio of the building decreased from 14.48% to 2.90%. This scenario has the potential to decrease the thermal conductivity through the wall by 58%. Consequently, there appears to be a substantial decrease in heat loss through the walls.

Extreme weather phenomena, such as variations in temperature due to global warming and the greenhouse effect, fluctuations in relative humidity caused by changes in precipitation patterns, floods, and rising sea levels, as well as changes in air velocity caused by hurricanes, typhoons, and tornadoes, are among the primary indicators used to characterize future climate change. Both historic and contemporary buildings are particularly vulnerable to this climatic impact. They experience the negative impacts of the heightened fluctuations and alterations in temperature, precipitation, and soil moisture. Additionally, their construction materials undergo degradation and a loss of strength [48]. If the building has structural issues, experiences seasonal effects, or encounters extreme weather conditions, the electro-osmosis system alone, which is designed to prevent capillary moisture, will not be effective in controlling the significant water inflow. To address such situations, it is advisable to first prevent the influx of large amounts of water and subsequently implement an electro-osmosis system, which offers a more reliable and assured solution.

For more comprehensive scientific research, it is advisable to assess the impact of a capillary moisture repulsion system on building energy consumption and cost-effectiveness using a life cycle analysis.

Author Contributions: Conceptualization, A.K. and M.N.U.; Data Curation, E.Y. and A.K.; Investigation, A.K., E.Y. and M.N.U.; Methodology, A.K. and M.N.U.; Administration, A.K. and M.N.U.; Writing—Original Draft Preparation, A.K., E.Y. and M.N.U.; Writing—Review and Editing, A.K., E.Y. and M.N.U. All authors have read and agreed to the published version of the manuscript.

Funding: The research received financial support from Unico Bina Enerji Çözümleri San. ve Tic. A.S. company (İstanbul, Türkiye).

Data Availability Statement: Data are contained within the article.

Acknowledgments: We extend our sincere gratitude to the company Mir Arastırma ve Geliştirme Inc. (İstanbul, Türkiye) for their invaluable technical support.

Conflicts of Interest: The authors declare no conflicts of interest. The funders had no role in the design of the study; in the collection, analyses, or interpretation of data; in the writing of the manuscript; or in the decision to publish the results.

References

1. Franzoni, E. State-of-the-art on methods for reducing rising damp in masonry. *J. Cult. Herit.* **2018**, *31*, S3–S9. [CrossRef]
2. Sandrolini, F.; Franzoni, E. An operative protocol for reliable measurements of moisture in porous materials of ancient buildings. *Build. Environ.* **2006**, *41*, 1372–1380. [CrossRef]
3. Vos, B.H. Suction of Groundwater. *Stud. Conserv.* **2014**, *16*, 129–144. [CrossRef]
4. Yousuf, H.; Al-Kheetan, M.J.; Rahman, M.M.; Ghaffar, S.M.; Braimah, N.; Chamberlain, D.A. Introducing a novel concept of wick drainage in masonry structures. *J. Build. Eng.* **2022**, *51*, 104332. [CrossRef]
5. Al-Kheetan, M.J.; Rahman, M.M.; Chamberlain, D.A. Remediation and protection of masonry structures with crystallising moisture blocking treatment. *Int. J. Build. Pathol. Adapt.* **2018**, *36*, 77–92. [CrossRef]
6. Lieff, M.; Trechsel, H.R. *Moisture Migration in Buildings: A Symposium*; ASTM: West Conshohocken, PA, USA, 1982.
7. Karoglou, M.; Moropoulou, A.; Giakoumaki, A.; Krokida, M.K. Capillary rise kinetics of some building materials. *J. Colloid Interface Sci.* **2005**, *284*, 260–264. [CrossRef] [PubMed]
8. Jiménez-González, I.; Rodríguez-Navarro, C.; Scherer, G.W. Role of clay minerals in the physicomechanical deterioration of sandstone. *J. Geophys. Res. Earth Surf.* **2008**, *113*, 1–17. [CrossRef]
9. Kim, R.L.; Tore, K.; Hans, O.H.; Jan, V.T.; Knut, H. A frost decay exposure index for porous, mineral building materials. *Build. Environ.* **2007**, *42*, 3547–3555.
10. Franzoni, E.; Sassoni, E. Correlation between microstructural characteristics and weight loss of natural stones exposed to simulated acid rain. *Sci. Total Environ.* **2011**, *412–413*, 278–285. [CrossRef]
11. Pleyers, G.J. Treatment of rising damp in wet conditions with new hydrophobic pore filling resins. In *Hydrophobe III, Proceedings of the 3rd International Conference on Surface Technology with Water Repellent Agents, Universität Hannover, Hannover, Germany, 25–26 September 2001*; Aedificatio Verlag: Freiburg, Germany, 2001; pp. 247–256.
12. Salmon, D.R.; Williams, R.G.; Tye, R.P. Thermal Conductivity and Moisture Measurements on Masonry Materials. In *Insulation Materials: Testing and Applications*; ASTM International: West Conshohocken, PA, USA, 2002; Volume 4, pp. 58–75.
13. Gentilini, C.; Franzoni, E.; Bandini, S.; Nobile, L. Salt Attack Effects on the Shear Behavior of Masonry: Preliminary Results of an Experimental Campaign. *Key Eng. Mater.* **2017**, *747*, 512–517. [CrossRef]
14. Franzoni, E. Rising damp removal from historical masonries: A still open challenge. *Constr. Build. Mater.* **2014**, *54*, 123–136. [CrossRef]
15. Bertolini, L.; Coppola, L.; Gastaldi, M.; Redaelli, E. Electroosmotic transport in porous construction materials and dehumidification of masonry. *Constr. Build. Mater.* **2009**, *23*, 254–263. [CrossRef]
16. Collepardi, M. Degradation and restoration of masonry walls of historical buildings. *Mater. Struct.* **1990**, *23*, 81–102. [CrossRef]
17. Heiman, J.L. An Evaluation of Methods of Treating Rising Damp. In *Moisture Migration in Buildings*; ASTM International: West Conshohocken, PA, USA, 1982; pp. 121–137.
18. Hampel, C.A. *The Encyclopedia of Electrochemistry*; Reinhold Pub. Corp.: New York, NY, USA, 1964.
19. Azzam, R.; Oey, W. The Utilization of Electrokinetics in Geotechnical and Environmental Engineering. *Transp. Porous Media* **2001**, *42*, 293–314. [CrossRef]
20. Andrade, C.; Castellote, M.; Sarria, J.; Alonso, C. Evolution of pore solution chemistry, electro-osmosis and rebar corrosion rate induced by realkalisation. *Mater. Struct.* **1999**, *32*, 427–436. [CrossRef]
21. Casagrande, L. Electro-Osmotic Stabilization of soils. *J. Boston Soc. Civil Eng.* **1952**, *39*, 51–83.
22. Paz-García, J.M.; Johannesson, B.; Ottosen, L.M.; Alshawabkeh, A.N.; Ribeiro, A.B. Modeling of electrokinetic desalination of bricks. *Electrochim. Acta* **2012**, *86*, 213–222. [CrossRef]

23. Sharpe, R.W. Injection systems for damp-proofing. *Build. Environ.* **1977**, *12*, 191–197. [CrossRef]
24. Young, D. *Salt Attack and Rising Damp: A Guide to Salt Damp in Historic and Older Buildings*; Heritage Council of NSW, Heritage Victoria, South Australian Department for Environment and Heritage, Adelaide City Council: Kilkenny, UK, 2008.
25. Torres, I.; de Freitas, V.P. The influence of the thickness of the walls and their properties on the treatment of rising damp in historic buildings. *Constr. Build. Mater.* **2010**, *24*, 1331–1339. [CrossRef]
26. Zhang, X.; Nowamooz, H. Effect of rising damp in unstabilized rammed earth (URE) walls. *Constr. Build. Mater.* **2021**, *307*, 124989. [CrossRef]
27. Pratiwi, S.N.; Wijayanto, P.; Putri, C.A. Diagnosis of capillary rise in heritage building. *IOP Conf. Ser. Earth Environ. Sci.* **2021**, *780*, 012076. [CrossRef]
28. Goudjil, N.; Vanhove, Y.; Djelal, C.; Kada, H. Electro-Osmosis Applied for Formwork Removal of Concrete. *J. Adv. Concr. Technol.* **2012**, *10*, 301–312. [CrossRef]
29. Peruzzi, R.; Poli, T.; Toniolo, L. The experimental test for the evaluation of protective treatments: A critical survey of the "capillary absorption index". *J. Cult. Herit.* **2003**, *4*, 251–254. [CrossRef]
30. Tomašić, I.; Lukić, D.; Peček, N.; Kršinić, A. Dynamics of capillary water absorption in natural stone. *Bull. Eng. Geol. Environ.* **2011**, *70*, 673–680. [CrossRef]
31. Washburn, E.W. The Dynamics of Capillary Flow. *Phys. Rev.* **1921**, *17*, 273–283. [CrossRef]
32. Rirsch, E.; Zhang, Z. Rising damp in masonry walls and the importance of mortar properties. *Constr. Build. Mater.* **2010**, *24*, 1815–1820. [CrossRef]
33. Lu, J.; Wang, K.; Qu, M.-L. Experimental determination on the capillary water absorption coefficient of porous building materials: A comparison between the intermittent and continuous absorption tests. *J. Build. Eng.* **2020**, *28*, 101091. [CrossRef]
34. Çelik, M.Y.; Sert, M. An assessment of capillary water absorption changes related to the different salt solutions and their concentrations ratios in the Döğer tuff (Afyonkarahisar-Turkey) used as building stone of cultural heritages. *J. Build. Eng.* **2021**, *35*, 102102.
35. Çelik, M.Y.; Köken, İ. The Effect of Temperature and Salty Water on the Capillary Water Absorption Capacity of Volcanic Rocks Used as Building Stones. *J. Innov. Civ. Eng. Technol.* **2023**, *5*, 17–47.
36. Çelik, M.Y.; Yılmaz, S. *Statik, Tuzlu ve Asidik sulu Ortamların Poroziteli Yapıtaşlarının Kapiler su Emme Potansiyeline Etkisi*; Gazi Üniversitesi Mühendislik-Mimarlık Fakültesi Dergisi: Ankara, Turkey, 2018; pp. 611–628.
37. Karagiannis, N.; Karoglou, M.; Bakolas, A.; Krokida, M.; Moropoulou, A. The influence of dynamic environmental conditions on capillary water uptake of building materials. *J. Build. Phys.* **2018**, *42*, 506–526. [CrossRef]
38. Torres, M.I.M.; de Freitas, V.P. Modelling of rising damp in historical buildings. In *Historical Constructions. Possibili-Ties of Numerical and Experimental Techniques, Proceedings of the 3rd International Seminar, Guimaraes, Portugal, 7–9 November 2001*; Lourenço, P.B., Roca, P., Eds.; University of Minho: Guimarães, Portugal, 2001; pp. 381–390.
39. Holm, A.; Künzel, H.M. Two-dimensional transient heat and moisture simulations of rising damp with WUFI2d. In *Research in Building Physics*; CRC Press: Boca Raton, FL, USA, 2020; pp. 363–367.
40. Baker, P.H.; Bailly, D.; Campbell, M.; Galbraith, G.H.; McLean, R.C.; Poffa, N.; Sanders, C.H. The application of X-ray absorption to building moisture transport studies. *Measurement* **2007**, *40*, 951–959. [CrossRef]
41. Mirline. What Is the Application Process: Moisture and Desalt Removal Technology. 7 March 2021. Available online: https://www.mirline.com/sistemimiz/uygulama-sureci-nasildir (accessed on 15 December 2023).
42. Merkezi, T.İ.A. *TDV İslâm Ansiklopedisi*; Türkiye Diyanet Vakfı (TDV): Ankara, Turkey, 1988; Available online: https://islamansiklopedisi.org.tr/gul-camii (accessed on 15 December 2023).
43. GANN. GANN Handbook 30 (HB30). Available online: https://www.gann.de/_Resources/Persistent/71d36426de8dc0f29a5365dc197efe99841a380c/HB30_EN.pdf (accessed on 15 December 2023).
44. Chassagne, R.; Dörfler, F.; Guyenot, M.; Harting, J. Modeling of capillary-driven flows in axisymmetric geometries. *Comput. Fluids* **2019**, *178*, 132–140. [CrossRef]
45. *BS EN 1925:1999*; Natural Stone Test Methods. Determination of Water Absorption Coefficient By Capillarity. British Standards Institution (BSI): London, UK, 15 August 1999.
46. Adan, O.C.G.; Eindhoven, T.U. *On the Fungal Defacement of Interior Finishes*; Eindhoven University of Technology: Eindhoven, The Netherlands, 1994.
47. Gawin, D.; Kośny, J.; Desjarlais, A.O. Effect of Moisture on Thermal Performance and Energy Efficiency of Buildings with Lightweight Concrete Walls. *Commer. Build. J. Technol. Des. Perform. Anal.* **2000**, *3*, 149–159. Available online: https://www.eceee.org/library/conference_proceedings/ACEEE_buildings/2000/Panel_3/p3_12/ (accessed on 15 December 2023).
48. D'Ayala, D.; Aktas, Y.D. Moisture dynamics in the masonry fabric of historic buildings subjected to wind-driven rain and flooding. *Build. Environ.* **2016**, *104*, 208–220. [CrossRef]

Disclaimer/Publisher's Note: The statements, opinions and data contained in all publications are solely those of the individual author(s) and contributor(s) and not of MDPI and/or the editor(s). MDPI and/or the editor(s) disclaim responsibility for any injury to people or property resulting from any ideas, methods, instructions or products referred to in the content.